# MULTISTATIC PASSIVE RADAR IMAGING USING THE SMOOTHED PSEUDO WIGNER-VILLE DISTRIBUTION

*Yong Wu and David C. Munson, Jr.*

Coordinated Science Lab and Department of Electrical and Computer Engineering
University of Illinois at Urbana-Champaign
Urbana, IL, 61801
yongwu@uiuc.edu, d-munson@uiuc.edu

## ABSTRACT

We investigate passive radar imaging of aircraft using reflected TV signals. We apply a Smoothed Pseudo Wigner-Ville Distribution (SPWVD)-based SAR imaging algorithm to two different scenarios. In the first simulation, multistatic VHF-band dataset generated by Fast Illinois Solver Code (FISC) is used. In the second simulation, a more realistic simulated passive radar dataset is used. A set of instantaneous images are produced by our algorithm, which have higher resolution and show more detail and features of the aircraft than can be obtained by Direct Fourier Reconstruction (DFR). The set of images provides visually more information about the target and helps to estimate its shape and features. This study suggests that the SPWVD-based imaging might be useful in passive radar imaging and target classification.

## 1. INTRODUCTION

We are investigating passive imaging of aircraft using reflected radio or TV signals. The problem is multistatic: there is one receiver and multiple transmitters. The receiver collects radio or TV signals reflected off the target. As the plane flies by, multiple broadcasting stations can provide data with frequency and angular diversity for image reconstruction [1, 2, 6]. The bistatic frequency coverage is lower than for a conventional X-band SAR. Thus the image resolution is potentially quite low. If narrow-angle data is used, the cross-range resolution may be so poor that the reconstructed image is unrecognizable. Thus wide-angle data is needed to achieve acceptable cross-range resolution. This raises the issue of aspect-dependent scattering of aircraft [3, 4]. Within a wide-angle observation aperture, the reflectivity may change with aspect dramatically. We have shown that Direct Fourier Reconstruction (DFR) in aspect-dependent imaging gives blurred images [5] . We proposed an imaging algorithm using the Smoothed Pseudo Wigner-Ville distribution (SPWVD) and showed analytically that it produces better images than DFR. We also studied passive imaging using the actual frequencies and locations of TV transmitters in the Gaithersburg, MD area. We demonstrated that useful images can be formed from the data using DFR [6].

In this paper, we first apply our SPWVD-based imaging algorithm to a multistatic dataset at VHF-band to generate several instantaneous images of an aircraft. We also apply the algorithm to a more realistic dataset obtained by simulating a passive radar and obtained instantaneous images which look better than those obtained by DFR. SPWVD-based imaging shows more features of the target, thus providing more information for classification.

This work is supported by DARPA under the contract number F49620-98-1-0498

## 2. SPWVD-BASED SAR IMAGING

In this section, we review the main results of our previous work on SPWVD-based SAR imaging [5]. In DFR processing, polar format data is interpolated to a rectangular grid and an inverse Fourier transform is used to reconstruct the image [7, 8]. Consider two point targets at $(x_0, y_0)$ and $(x_1, y_1)$. If the two points' brightnesses vary with aspect, the reflectivity becomes $f(x, y, \theta) = \delta(x - x_0, y - y_0)e^{-\frac{(\theta-\theta_0)^2}{c_0}} + \delta(x - x_1, y - y_1)e^{-\frac{(\theta-\theta_1)^2}{c_1}}$, where we assume that the scattering amplitude varies with aspect according to a Gaussian profile. $\theta_i$ is the angle of maximum brightness. The collected Fourier data is $\tilde{F}(u, v) = e^{-j(ux_0+vy_0)}e^{-\frac{(u-a_0)^2}{b_0}} + e^{-j(ux_1+vy_1)}e^{-\frac{(u-a_1)^2}{b_1}}$, where $u = k\theta$, $k$ is a constant. If Fourier inversion is used and the bandwidth available is wide, the reconstructed image is

$$\begin{aligned}\tilde{f}(x, y) &= \delta(y - y_0)e^{-b_0(x-x_0)^2}e^{ja_0\sqrt{b_0}(x-x_0)} + \\ &\quad \delta(y - y_1)e^{-b_1(x-x_1)^2}e^{ja_1\sqrt{b_1}(x-x_1)} \quad (1)\end{aligned}$$

where $*_x$ stands for convolution in x. In the $x$ direction, the $\delta$ functions are spread out and the complex multiplier may cause cancelation of the two signals. Hence, it may be impossible to even detect the two targets, and the resulting image quality may be severely degraded. This analysis can be extended to multiple point targets for an aircraft scattering-center model, suggesting that DFR applied to wide-angle data could degrade image quality.

To solve this problem, we have considered using the Wigner-Ville distribution(WVD) [9, 10] in the cross-range direction to replace the inverse Fourier transform. The cross-terms can be suppressed by using the SPWVD. We can model an aircraft using a scattering-center model with aspect dependent reflectivity: $f(x,y,\theta) = \sum_{i=0}^{N} A_i \delta(x - x_i, y - y_i) e^{-\frac{(\theta-\theta_i)^2}{c_i}}$. Applying the SPWVD, a sequence of images can be produced:

$$\tilde{f}(x,y,u) = [(\sum_{i=0}^{N} A_i B \sqrt{\frac{2\pi}{b_i}} sinc[B(y-y_i)] \\ (B-2 \mid u \mid)\{sinc[(x-x_i)(B-2 \mid u \mid)] *_x e^{-2b_i x^2}\} \\ e^{-\frac{2\pi^2}{b_i}(u-a_i)^2}) *_u q(u)] *_x h(x) \quad (2)$$

where $\mid u \mid \leq B/2$ and $q(\cdot)$ and $h(\cdot)$ are the smoothing window functions (e.g. Hamming windows). Symmetry enhancement can be used to improve image recognizability to human eyes since the target is known to be symmetric. By this, we mean that the maximum magnitude of the two symmetric pixels in the image is assigned as the value for both pixels.

*Steps of the proposed imaging algorithm:*

*1. Interpolate Fourier data to rectangular grid;*

*2. Apply FFT in range direction;*

*3. Apply SPWVD in cross-range direction to generate a sequence of images;*

*4. (Optional) Combine instantaneous images into one image;*

*5. (Optional) Apply symmetry enhancement for viewing.*

Since the SPWVD is always real, the shift in the weighting function does not produce a complex multiplication term in the result, thus avoiding the cancelation of neighboring points. The SPWVD also ensures that only the subset of scatterers visible at a certain aspect are shown in the corresponding instantaneous image ( weighted by the weighting functions). SPWVD-based image formation yields a sequence of instantaneous images that show the reflectivity of the target as a function of aspect. The instantaneous images can be combined into one image when the resolution is high, as we did in [5] for L-band monostatic data generated by XPATCH. For low frequency (e.g. VHF band) multistatic data, the resolution is low and we find that it might not be advantageous to combine these instantaneous images into one image. However, the instantaneous images show different features of the target from different aspects, with better resolution than those obtained by DFR. Thus the set of images can provide more information about the target than a single DFR image.

## 3. SIMULATION USING A COMPLETE MULTISTATIC DATASET

We used Fast Illinois Solver Code (FISC) to simulate electromagnetic returns from a Falcon-100 aircraft model. Figure 2(a) shows an optical image of the aircraft. In the simulations, a single incident frequency, 79.25 MHz, was assumed. The incident direction were $-90^o$ to $90^o$, in steps of $5^o$. The aircraft was oriented in the $90^o$ direction. Receivers were located around the target from $0^o$ to $360^o$ with a spacing of $1^o$. The Fourier domain coverage is illustrated in Figure 1. Each circle represents data for one incident direction. HH polarization was used. From this full dataset, we chose 2 subsets ($-15$ to 25 degrees and $-15$ to 45 degrees) to test our image reconstruction methods. Fourier data was interpolated to a rectangular grid, and then processed using DFR. Symmetry enhancement was applied. Figures 2(b) and (c) show the images obtained using DFR with 40 and 60 degree wide data. We can see that the image from 60 degrees of data has higher cross-range resolution since the synthetic aperture is larger. The 60 degree data was processed using SPWVD-based imaging to produce several instantaneous images. These images are shown in Figures 2(d), (e) and (f). They have higher resolution and show different features as aspect changes. The contour and shape of the aircraft is clearer, and they also show some features not visible in the images given by DFR in Fig. 2(c).

## 4. IMAGING USING A REALISTIC SIMULATED PASSIVE RADAR DATASET

We considered a passive radar scenario using TV transmitter frequencies and locations in the Gaithersburg, MD area [6]. Figure 3 illustrates the locations of the TV stations, receiver, and flight path. We used 21 TV channels (5, 7, 9, 11, 13, 14, 20, 22, 24, 26, 30, 34, 38, 39, 41, 45, 48, 51, 58, 61, 67). The large box in Figure 4(a) shows the sparse Fourier data grid. The origin of the Fourier space is at the center bottom of the figure. Using FISC, we simulated the Fourier data only within a semicircular region within the smaller box shown in Fig. 4(b). The grid inside the smaller box corresponds to the data that could be generated with a 211.25 MHz signal. The larger data grid would require frequencies up to 800 MHz . Since we were unable to generate the higher frequency data, our image reconstruction used only the data from the 21 channels that falls within the smaller box. All higher-frequency data was assumed to be zero. Thus, our simulations used only a small fraction of the data

that would be available in practice from the 21 channels. As a result, the images that we present below provide a loose lower bound on the quality that could be expected from a real system.

As a benchmark, we first used a 170 degree-wide complete FISC dataset ($-30^o$ to $140^o$ in Fig. 1) on a uniform grid, densely covering a semicircular area within the box in Fig. 4(b). The image obtained by DFR is shown in Fig. 5 (a). No symmetry enhancement was used in this experiment. The dataset was dense and, therefore, there was no interpolation error. This image shows that the aircraft is heading toward the top left corner in the figure and we can use it as 'ground truth'. We then took the sparse data on the nonuniform grid in Fig. 4(b) and interpolated it to a uniform rectangular grid using the *griddata* function provided in MATLAB. The interpolated data was processed by DFR to give the image shown in Fig. 5(b). There is considerable degradation in the image obtained by DFR due to the interpolation error in the Fourier domain. The right wing and the tail are obscure. Four instantaneous images obtained by processing the interpolated data using SPWVD-based imaging are shown in Fig. 5 (c) - (f). The instantaneous images have better resolution and together show more detail of the aircraft, compared to Fig. 5(b). In (c), more detail of the wings is visible. (d) shows a strong reflection from the left wing, which becomes weaker in (e) and (f). The tail shape is more visible in (d), (e) and (f). In (f), the right engine is visible. The overall shape of the aircraft can be estimated from these instantaneous images. This provides more information than a DFR image alone. We believe that SPWVD-based imaging might be helpful for classification.

## 5. ACKNOWLEDGMENT

We thank Dr. Aaron Lanterman for generating the FISC data used in our simulations.

## 6. REFERENCES

[1] D. L. Mensa and G. R. Heidbreder, "Bistatic synthetic-aperture radar imaging of rotating objects," *IEEE Trans. Aerosp Electron Syst.*, vol. 18, no. 4, pp. 423–431, Jul 1982.

[2] O. Arikan and D. C. Munson Jr., "A tomographic formulation of bistatic synthetic aperture radar," *Proceedings of ComCon 88, Advances in Communications and Control Systems, Baton Rouge, LA*, Oct 19-21 1988.

[3] B. D. Steinberg, "Microwave imaging of aircraft," *Proc. IEEE*, vol. 76, no. 12, pp. 1578–1592, Dec 1988.

[4] M. J. Gerry and L.C. Potter, "A parametric model for synthetic aperture radar measurements," *IEEE Trans. Antennas Propagat.*, vol. 47, no. 7, pp. 1179–1188, Jul 1999.

[5] Y. Wu and D. C. Munson Jr., "Wide-angle ISAR passive imaging using smoothed pseudo Wigner-Ville distribution," *in Proc. of the IEEE Radar Conference*, Atlanta, GA, May 1-3 2001.

[6] Y. Wu and D. C. Munson Jr., "Multistatic synthetic aperture imaging of aircraft using reflected television signals," *in Proc. of SPIE, Algorithms for synthetic aperture radar imagery VIII*, vol. 4382, Orlando, FL, Apr 16-19 2001.

[7] D. C. Munson Jr., J. D. O'Brien, and W. K. Jenkins, "A tomographic formulation of spot-light mode synthetic aperture radar," *Proc. IEEE*, vol. 71, no. 8, pp. 917–925, Aug 1983.

[8] C. C. Chen and H. C. Andrews, "Multifrequency imaging of radar turntable data," *IEEE Trans. Aerosp. Electron. Syst.*, vol. AES-16, no. 1, pp. 15–22, Jan 1980.

[9] L. Cohen, "Time-frequency distributions - a review," *Proc. IEEE*, vol. 77, no. 7, pp. 941–981, Jul 1989.

[10] V. C. Chen and S. Qian, "Joint time-frequency transform for radar range-Doppler imaging," *IEEE Trans. Aerosp. Electron. Syst.*, vol. 34, no. 2, pp. 486–499, Apr 1998.

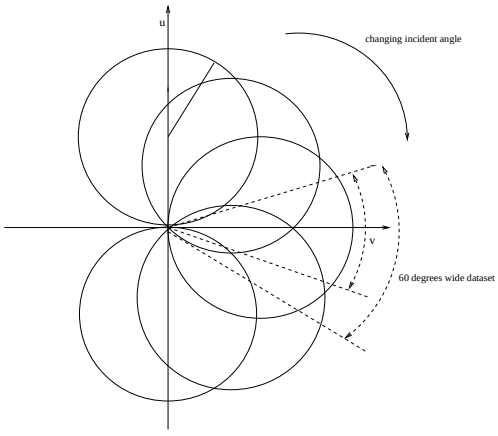


**Fig. 1**. The multistatic Fourier domain data coverage, generated using FISC.

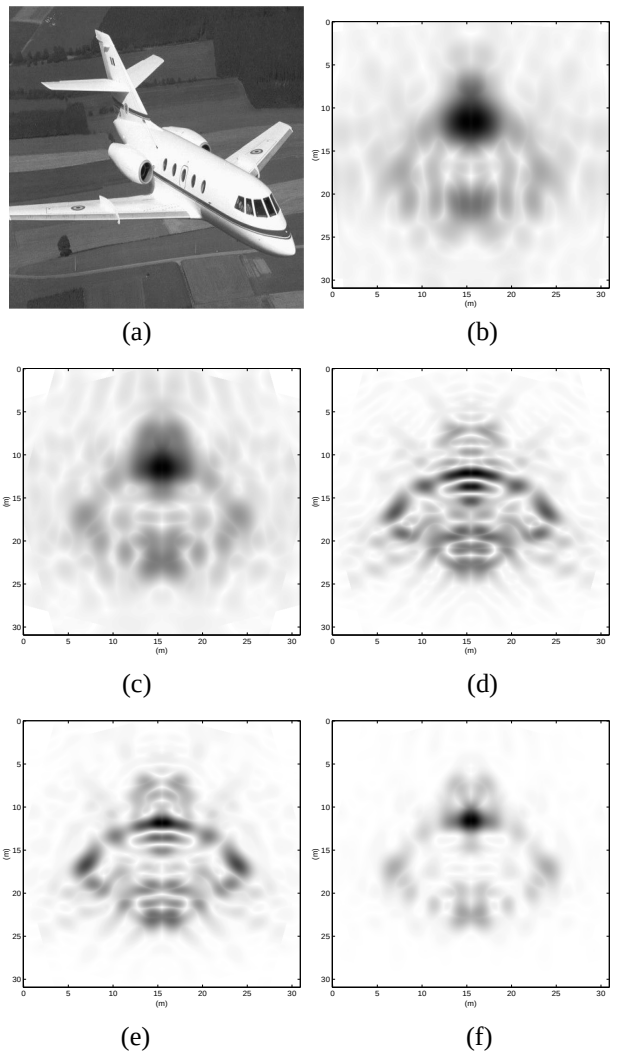

**Fig. 2**. Imaging from multistatic FISC data with Symmetry enhancement. (a) Optical image of Falcon-100 aircraft; (b) DFR image using 40 degree wide data;(c) DFR image using 60 degree wide data; (d) - (f): Instantaneous images produced by SPWVD using the 60 degree wide data.

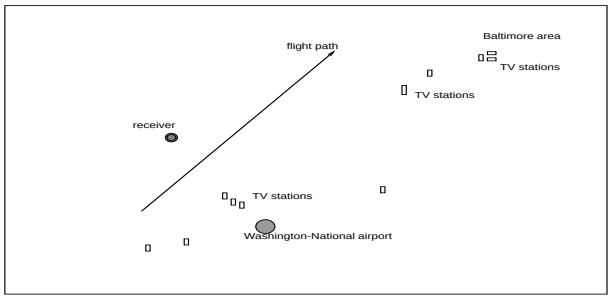


**Fig. 3**. Locations of the receiver, TV transmitters and target flight path, simulating a passive radar.

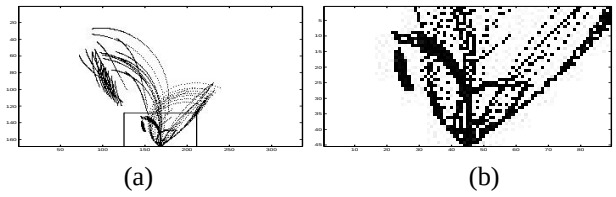

**Fig. 4**. (a) The nonuniform grid in Fourier space for the passive radar dataset obtained using 21 channels, for frequencies up to 800 MHz. (b) The grid inside the smaller box in (a), for frequencies up to 211.25 MHz only.

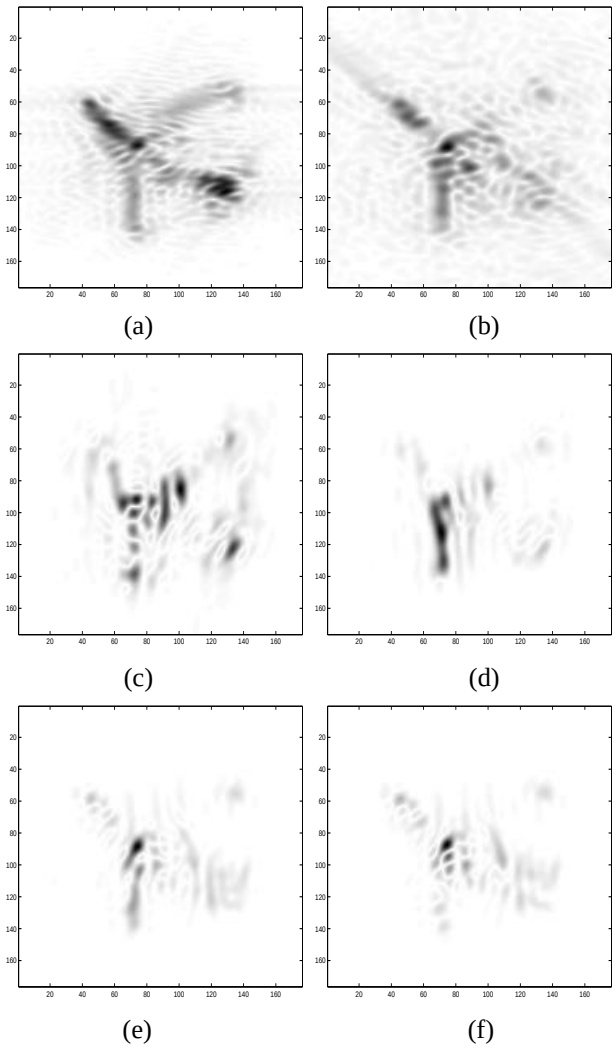

**Fig. 5**. Imaging from simulated passive radar data. (a):DFR image from the 170 degrees-wide complete dataset;(b) DFR image from the sparse simulated passive radar data; (c) - (f): Instantaneous images obtained by SPWVD-based imaging from the sparse simulated passive radar data.